Trigonal-Planar-Coordinated Organogold(I) Complexes Stabilized by Organometallic 1,4-Diynes: Reaction Behavior, Structure, and Bonding†

Katrin Köhler,‡ Sandro J. Silverio,§ Isabella Hyla-Kryspin,§ Rolf Gleiter,§,|| Laszlo Zsolnai,⊥ Alexander Driess,⊥ Gottfried Huttner,⊥,▽ and Heinrich Lang*,‡

Technische Universität Chemnitz, Institut für Chemie, Lehrstuhl Anorganische Chemie, Strasse der Nationen 62, D-09107 Chemnitz, Germany and Ruprecht-Karls-Universität Heidelberg, Organisch-Chemisches and Anorganisch-Chemisches Institut, Im Neuenheimer Feld 270, D-69120 Heidelberg, Germany

Received April 10, 1997⊗

The reaction of the bis(alkynyl) titanocenes [Ti](C≡CR^1)(C≡CR^2) ([Ti] = (η^5-$C_5H_4SiMe_3$)$_2$-Ti; **1a** R^1 = R^2 = $SiMe_3$; **1b** R^1 = R^2 = ^{t}Bu; **1c** R^1 = $SiMe_3$, R^2 = ^{t}Bu) with (C_5H_5N)$AuCl_3$ (**2**), LAuCl (**5a**, L = PPh_3; **5b**, L = SMe_2) as well as (Me_2S)AuR^3 (**6b**, R^3 = C≡C$SiMe_3$; **6c**, R^3 = C≡C^{t}Bu; **6d**, R^3 = $C_6H_2(CF_3)_3$-2,4,6; **6e**, R^3 = Me) is described. Treatment of [Ti](C≡C$SiMe_3$)$_2$ (**1a**) with (C_5H_5N)$AuCl_3$ (**2**) produces [Ti]Cl_2 (**3**) and Me_3SiC≡C−C≡C$SiMe_3$ (**4a**) together with Au(0). However, the linear two-coordinated gold(I) chlorides LAuCl (**5a**,**b**) react with **1a** to afford different products, depending on the Lewis bases applied. While in the reaction of the Ph_3P donor-stabilized gold(I) chloride **5a**, the titanocene dichloride (**3**) along with (Ph_3P)AuC≡C$SiMe_3$ (**6a**) is obtained, with the appropriate Me_2S donor-stabilized molecule **5b**, the titanocene dichloride (**3**) along with the heterobimetallic tweezer molecule {[Ti]-(C≡C$SiMe_3$)$_2$}AuC≡C$SiMe_3$ (**7a**) is formed. A possible mechanism for the different chemical behavior is discussed. Likewise, molecules of the latter type (compounds **7a**−**e**) can be synthesized in much better yields by the reaction of [Ti](C≡CR^1)(C≡CR^2) (**1a**−**c**) with (Me_2S)-AuR^3 (**6b**−**e**). In the heterobimetallic titanium−gold complexes {[Ti](C≡CR^1)(C≡CR^2)}AuR^3 (**7a**, R^1 = R^2 = $SiMe_3$, R^3 = C≡C$SiMe_3$; **7b**, R^1 = R^2 = ^{t}Bu, R^3 = C≡C^{t}Bu; **7c**, R^1 = $SiMe_3$, R^2 = ^{t}Bu, R^3 = C≡C$SiMe_3$; **7d**, R^1 = R^2 = $SiMe_3$, R^3 = $C_6H_2(CF_3)_3$-2,4,6; **7e**, R^1 = R^2 = $SiMe_3$, R^3 = Me), a low-valent monomeric organogold(I) moiety in a trigonal-planar environment is present, which is stabilized by the chelating effect of the organometallic π-tweezer bis(alkynyl) titanocene. The thermolysis of selected organogold(I) complexes affords, on elimination of the bis(alkynyl) titanocene fragment, the coupling products R^3−R^3 (**4**) and gold films. The X-ray structure analyses of compounds **7a**, **7b**, and **7d** are reported. It is found that in all compounds short titanium−gold bond lengths are present (**7a**, 3.007(2) Å; **7b**, 2.975(1) Å; **7d**, 2.995(1) Å). Calculations show that the complexation of the Au−R^3 monomers with the organometallic π-tweezer bis(alkynyl) titanocene is described by a four-center two-electron bond. The monomeric organogold(I) moieties are stabilized by a synergetic in-plane donation and back-donation of electron density between the bis(alkynyl) titanocene and the Au−R^3 species. A direct donor−acceptor Au−Ti interaction contributes to this stabilization.

Introduction

Gold(I) compounds are of interest both for synthetic use and physical applications: They can be used in organic and organometallic synthesis,[1] they are present in various antiarthritic and cancerostatic drugs,[2] and they are, for instance, of considerable interest due to the luminescence properties observed for trigonal-planar-coordinated gold(I) centers.[3] These compounds generally exist as aggregated AuX species (X = singly-bonded inorganic or organic ligand).[4] Nevertheless, they can be broken down to monomeric linear two-coordinate LAuX compounds by using Lewis bases L (*e.g.*, N-, P-, S-donor molecules).[4d,5] With their 14-valence electron count, they represent coordinatively unsaturated complexes. This coordination mode is most common in gold(I) chemistry and is realized in mono- (structural

† With deepest sympathy dedicated to Prof. Dr. Gottfried Huttner on the occasion of his 60th birthday.

‡ Technische Universität Chemnitz.

§ Ruprecht-Karls-Universität Heidelberg, Organisch-Chemisches Institut.

|| To whom correspondence pertaining to extended-Hückel and density functional theory calculations should be addressed.

⊥ Ruprecht-Karls-Universität Heidelberg, Anorganisch-Chemisches Institut.

▽ To whom correspondence pertaining to crystallographic studies should be addressed.

⊗ Abstract published in *Advance ACS Abstracts,* October 1, 1997.

(1) (a) Grandberg, K. I.; Dyadchenko, V. P. *J. Organomet. Chem.* **1994**, *474*, 1. (b) Armer, B.; Schmidbaur, H. *Angew. Chem., Int. Ed. Engl.* **1970**, *9*, 101. (c) Puddephatt, R. J. In *Comprehensive Organometallic Chemistry*; Wilkinson, G., Stone, F. G. A., Abel, E. W., Eds.; Pergamon: Oxford, 1982; Vol. 2, p 765. (d) Anderson, G. K. *Adv. Organomet. Chem.* **1982**, *20*, 39. (e) Puddephatt, R. J. *Gold Bull.* **1977**, *10*, 108. (f) Nesmeyanov, A. N.; Perevalova, E. G.; Grandberg, K. J.; Lemenovskii, D. A. *Izv. Akad. Nauk. SSSR, Ser. Khim.* **1974**, 1124.

(2) (a) Lewis, A. J.; Walz, D. T. *Prog. Med. Chem.* **1982**, *19*, 1. (b) Sadler, P. J. *Struct. Bonding (Berlin)* **1976**, *29*, 171. (c) Brown, D. H.; Smith, W. E. *Chem. Soc. Rev.* **1980**, *9*, 217. (d) Shaw, C. F.; Isab, A. A.; Hoeschele, J. D.; Starisch, M.; Jocke, J.; Schulteis, P.; Xiao, J. *J. Am. Chem. Soc.* **1994**, *116*, 2254. (e) Graham, G. C.; Champion, G. D.; Ziegher, J. B. *Inflammopharmacology* **1991**, *1*, 99.

S0276-7333(97)00302-6 CCC: $14.00

type **A** molecules), bi- (structural type **B** molecules), and tridentate donors (structural type **C** molecules).[1c,5c,6] In

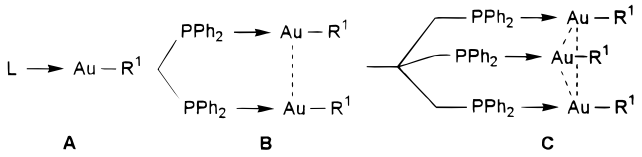

type **B** and **C** molecules, Au···Au interactions between the seemingly closed-shell group 11 metal centers is observed, which have recently attracted considerable attention.[5a,6] In addition to the usual coordination number of 2 with linear stereochemistry, there are only a few examples known of tetrahedral and trigonal-planar gold(I) complexes that have been structurally characterized.[7]

In this study, we describe the synthesis and chemical behavior as well as the structure and bonding of monomeric, alkyne-stabilized organogold(I) compounds, {[Ti](C≡CR^1)(C≡CR^2)}AuR^3 ([Ti] = (η^5-$C_5H_4SiMe_3$)$_2$Ti; R^1, R^2, R^3 = singly-bonded organic ligand) in which the gold atom possesses a trigonal-planar environment.

Results and Discussion

Reaction of [Ti](C≡CSiMe$_3$)$_2$ with LAuCl$_3$ and LAuCl. The bis(alkynyl) titanocene [Ti](C≡CSiMe$_3$)$_2$ (**1a**) ([Ti] = (η^5-$C_5H_4SiMe_3$)$_2$Ti)[8] reacts with 1 equiv of

Scheme 1. Possible Mechanism for the Formation of Compounds 1a, 3, and 6 as well as Compounds 3 and 7a

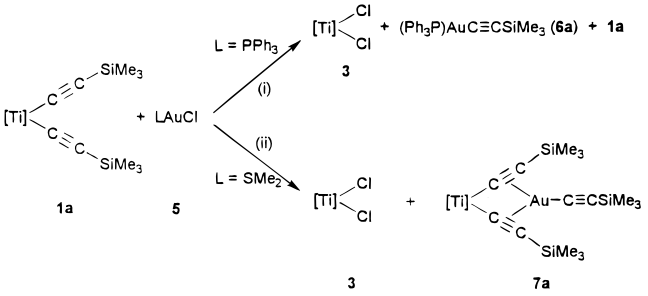

(C_5H_5N)AuCl$_3$ (**2**)[9] in tetrahydrofuran at 25 °C to yield a multitude of reaction products, of which [Ti]Cl$_2$ (**3**) as well as Me$_3$SiC≡C−C≡CSiMe$_3$ (**4a**) can be isolated, eq 1. It was noticed that the Schlenk flask was coated with

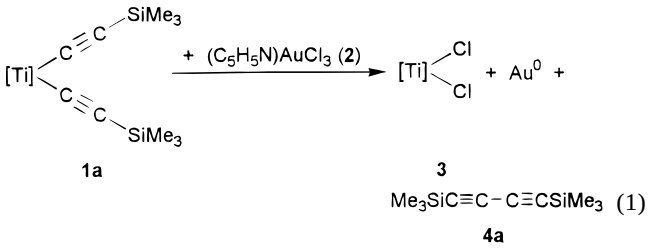

(1)

a thin gold film.

A similar observation is made on treatment of the organometallic penta-1,4-diyne **1a** with transition metal dichlorides of palladium, copper, and mercury.[10] In this respect, the formation of molecules [Ti]Cl$_2$ and Me$_3$SiC≡C−C≡CSiMe$_3$ (**4a**) along with the metals Pd, Cu, or Hg can plausibly be explained by an alkynyl−halide exchange reaction, producing **3** and M(C≡CSiMe$_3$)$_2$ at first, followed by reductive elimination of **4a** from M(C≡CSiMe$_3$)$_2$. In comparison to the latter finding, reductive elimination is suppressed when the donor-stabilized gold(I) chloride LAuCl (**5a**, L = PPh$_3$; **5b**, L = Me$_2$S) is reacted in tetrahydrofuran at 25 °C with the bis(alkynyl) titanocene **1a**. Depending on the Lewis bases L utilized different reaction products are produced: While **5a** affords **3** and (Ph$_3$P)AuC≡CSiMe$_3$ (**6a**) (reaction i, Scheme 1), **5b** yields **3** together with the heterobimetallic titanium−gold complex {[Ti](C≡CSiMe$_3$)$_2$}AuC≡CSiMe$_3$ (**7a**) (reaction ii, Scheme 1). A possible reaction pathway for the formation of the corresponding products obtained by treatment of **1a** with **5** is given in Scheme 2. It is likely that the reaction of the organometallic π-tweezer **1a** with **5b** is much faster compared with that using **5a**. This observation is in accord with the strength of the Lewis base L used. Seemingly, with Me$_2$S as the donor the heterobimetallic titanium−gold complex {[Ti](C≡CSiMe$_3$)$_2$}AuCl is formed first. In the step that follows, the gold-bonded chloride may undergo a nucleophilic attack at the titanium atom, giving rise to the formation of **6b** along with the monoalkynyl-substituted titanocene chloride intermediate [Ti](C≡CSiMe$_3$)(Cl) (**8**). Compound **8** redistributes

(3) (a) Li, D.; Hong, X.; Che, C. M.; Lo, W. C.; Peng, S. M. *J. Chem. Soc., Dalton Trans.* **1993**, 2929. (b) Hong, X.; Cheung, K. K.; Guo, C. X.; Che, C. M. *J. Chem. Soc., Dalton Trans.* **1994**, 1867. (c) Tzeng, B. C.; Lo, W. C.; Che, C. M.; Peng, S. M. *J. Chem. Soc., Chem. Commun.* **1996**, 181. (d) Müller, T. E.; Choi, S. W. K.; Mingos, D. M. P.; Murphy, D.; Williams, D. J.; Yam, V. W. W. *J. Organomet. Chem.* **1994**, *484*, 209. (e) Forward, J. M.; Bohmann, D.; Fackler, J. P.; Staples, R. J. *Inorg. Chem.* **1995**, *34*, 6330. (f) Yam, V. W. W.; Lee, W. K.; Lai, T. F. *Organometallics* **1993**, *12*, 2383. (g) Yam, V. W. W.; Chan, L. P.; Lai, T. F. *Organometallics* **1993**, *12*, 2197. (h) Yam, V. W. W.; Lee, W. K.; Lai, T. F. *J. Chem. Soc., Chem. Commun.* **1993**, 1517. (i) Yam, V. W. W.; Chan, L. P.; Lai, T. F. *J. Chem. Soc., Dalton Trans.* **1993**, 2075.

(4) (a) Schmidbaur, H.; Grohmann, A. in *Comprehensive Organometallic Chemistry II*; Elsevier Science: Oxford, 1995. (b) Schmidbaur, H. Organogold Compounds, *Gmelin Handbook of Inorganic Chemistry*; Springer Verlag: Berlin, 1980. (c) Mingos, D. M. P.; Yau, J.; Menzer, S.; Williams, D. J. *Angew. Chem., Int. Ed. Engl.* **1995**, *34*, 1894. (d) Mingos, D. M. P. *J. Chem. Soc., Dalton Trans.* **1996**, 561.

(5) (a) Gräfe, A.; Kruck, T. *J. Organomet. Chem.* **1996**, *506*, 31. (b) Müller, T. E.; Choi, S. W.; Mingos, D. M. P.; Murphy, D.; Williams, D. J.; Yam, V. W. W. *J. Organomet. Chem.* **1994**, *484*, 209. (c) Puddephatt, R. J. in *Comprehensive Coordination Chemistry*; Wilkinson, G., Gillard, R. G., McCleverty, J. A., Eds.; Pergamon Press: New York, 1987; Vol. 5, p 861. (d) Bruce, M. J.; Nicholson, B. K.; Shawkataly, O. B. *Inorg. Synth.* **1989**, *26*, 324. (e) Jia, G.; Puddephatt, R. J.; Scott, J. D.; Vittal, J. J. *Organometallics* **1993**, *12*, 3565. (f) Irwin, M. J.; Jia, G.; Payne, N. C.; Puddephatt, R. J. *Organometallics* **1996**, *15*, 51. (g) Yang, Y.; Ramamoothy, V.; Sharp, P. R. *Inorg. Chem.* **1993**, *32*, 1946.

(6) (a) Payne, N. C.; Ramachandran, R.; Puddephatt, R. J. *Can. J. Chem.* **1995**, *73*, 6. (b) Li, D.; Hong, X.; Che, C. M.; Lo, W. C.; Peng, S. M. *J. Chem. Soc., Dalton Trans.* **1993**, 2929. (c) Schmidbaur, H.; Wohlleben, A.; Schubert, U.; Frank, A.; Huttner, G. *Chem. Ber.* **1977**, *110*, 2751. (d) Schmidbaur, H.; Herr, R.; Müller, G.; Riede, J. *Organometallics* **1985**, *4*, 1208. (e) Cooper, M. K.; Henrick, K.; McPartlin, M.; Latten, J. L. *Inorg. Chim. Acta* **1982**, *65*, 185. (f) Fernandez, E. J.; Gimeno, M. C.; Jones, P. G.; Laguna, A.; Laguna, M.; Lopez-de-Luzuriaga, J. M.; Rodriguez, M. A. *Chem. Ber.* **1995**, *128*, 121.

(7) (a) Guggenberger, L. J. *J. Organomet. Chem.* **1974**, *81*, 271. (b) Jones, P. G. *J. Chem. Soc., Chem. Commun.* **1980**, 1031. (c) Vicente, J.; Arcas, A.; Jones, P. G.; Lautner, J. *J. Chem. Soc., Dalton Trans.* **1990**, 451. (d) Cerrada, E.; Jones, P. G.; Laguna, A.; Laguna, M. *Inorg. Chem.* **1996**, *35*, 2995. (e) Baenziger, N. C.; Dittemore, K. M.; Doyle, J. R. *Inorg. Chem.* **1974**, *13*, 805. (f) Huffman, J. C.; Roth, R. S.; Siedle, A. R. *J. Am. Chem. Soc.* **1976**, 4340.

(8) (a) Lang, H.; Herres, M.; Zsolnai, L. *Organometallics* **1993**, *12*, 5008. (b) Lang, H.; Seyferth, D. *Z. Naturforsch.* **1990**, *45b*, 212. For related (η^5-C_5H_5)$_2$Ti(C≡CSiMe$_3$)$_2$, see: Wood, G. L.; Knobler, C. B.; Hawthorne, M. F. *Inorg. Chem.* **1989**, *28*, 382.

(9) (a) Peshchevitskii, B. I.; Konovalova, V. S. *Russ. J. Inorg. Chem.* **1971**, *16*, 69. (b) Belli Dell'Amico, D.; Calderazzo, F. *Gazz. Chim. Ital.* **1973**, *103*, 1099.

(10) (a) Frosch, W. Diploma-Thesis, University of Heidelberg, Heidelberg, Germany, 1995. (b) Köhler, K. Ph.D. Thesis, University of Heidelberg, Heidelberg, Germany, 1996.

Scheme 2. Reaction of [Ti](C≡CSiMe$_3$)$_2$ (1a) with LAuCl[a]

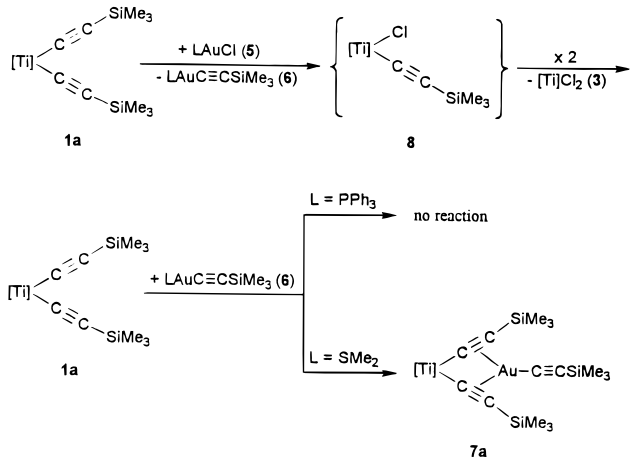

[a] **5a**, L = PPh$_3$; **5b**, L = Me$_2$S.

in solution, producing **3** together with **1a**.[11] The latter compound reacts with the earlier-formed (Me$_2$S)-AuC≡CSiMe$_3$ (**6b**), which upon displacement of the Lewis base Me$_2$S by the two alkynyl ligands of the 3-titano-1,4-diyne **1a**, yields the heterobimetallic complex {[Ti](C≡CSiMe$_3$)$_2$}AuC≡CSiMe$_3$ (**7a**) (Schemes 1 and 2). Moreover, the formation of **7a** supports the above-described initial step in which **1a** and **5b** afford the titanium−gold complex {[Ti](C≡CSiMe$_3$)$_2$}AuCl.

However, the proposed mechanism for the formation of compounds **3** and **7a** on treatment of **1a** with **5b** is not applicable for **5a**: Although molecule **3** could be isolated, it is found that the alkynyl ligands of the additionally produced organometallic π-tweezer **1a** are not suitable for replacing the Ph$_3$P building block in **6a** (Schemes 1 and 2). Consequently, **1a** and **6a** could be separated. This pattern of chemical behavior can be explained by the stronger Lewis base Ph$_3$P, as compared with Me$_2$S. In conclusion, in the case of **5a**, the initial step is presumably a nucleophilic attack of the chloride ligand at the titanium atom with elimination of **6a**.

A similar product distribution to that found in the reaction of **1a** with **5b** is also obtained on treatment of **1a** with *in-situ*-generated copper(I) fluoride (Scheme 2).[12] In this reaction, {[Ti](C≡CSiMe$_3$)$_2$}CuC≡CSiMe$_3$, [Ti]F$_2$, and $^1/_n$[CuC≡CSiMe$_3$]$_n$ are generated. Moreover, compounds of the type [Ti](C≡CR)(Cl) (R = singly-bonded organic ligand) (**8**) are known and they undergo redistribution in solution, forming [Ti]Cl$_2$ and [Ti]-(C≡CR)$_2$.[11]

To support the intermediate formation of **8**, as postulated in Scheme 2, the 3-titano-1,4-pentadiyne was subsequently reacted with **5b** and LiC≡C^{t}Bu (**9a**) in diethyl ether at 0 °C, eq 2. The heterobimetallic titanium−gold compound {[Ti](C≡CSiMe$_3$)(C≡C^{t}Bu)}-AuC≡CSiMe$_3$ (**7c**), which contains different alkynyl ligands at the titanocene fragment, could be isolated in 60% yield. This finding supports the intermediate formation of **8** (Scheme 2), which then reacts with added **9a** to yield **1c**; **3** could be detected under the reaction conditions applied. Subsequently, the organometallic 1,4-diyne **1c** reacts with the earlier-generated compound

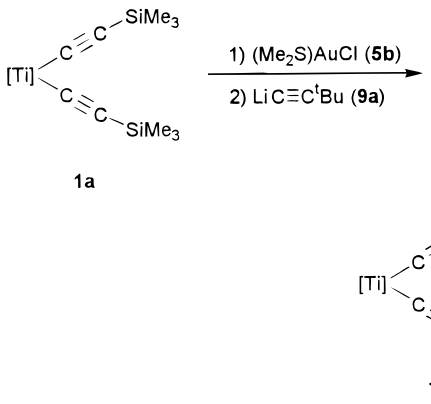

(2)

6b (Scheme 2) with elimination of Me$_2$S to form the titanium−gold compound **7c**.

Reaction of [Ti](C≡CR^1)(C≡CR^2) (1) with LAuR^3 (6). As already discussed, two-coordinate triphenylphosphane-stabilized organogold(I) compounds show no tendency to react with the organometallic π-tweezer **1**. Nevertheless, dimethylsulfane-stabilized organogold(I) compounds, (Me$_2$S)AuR^3, which contain a weaker Lewis base as compared to (Ph$_3$P)AuR^3, are suitable to synthesize heterobimetallic titanium−gold(I) compounds in which the gold atom possesses a trigonal-planar environment.

The bis(alkynyl) titanocenes **1a**−**c** react with an 1 molar equiv of the dimethylsulfane gold(I) compounds **6b**−**e** in diethyl ether at −70 to 0 °C on elimination of Me$_2$S to form pale orange heterobimetallic **7** in 60−80% yield (Table 1), eq 3. Appropriate purification of prod-

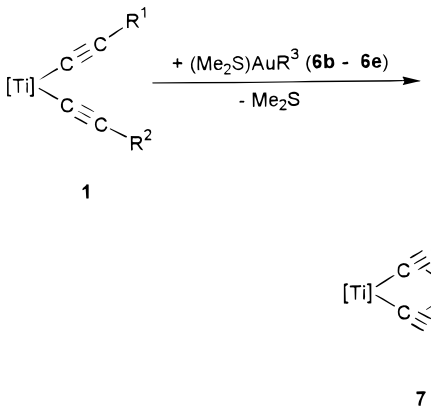

(3)

ucts **7a**−**e** gave pale orange crystals, which are stable for months in the solid state. They are soluble in most common organic solvents, such as *n*-pentane, toluene, diethyl ether, and tetrahydrofuran. In the solid state they can be handled in air for short periods, while in solution they slowly start to decompose.

Compounds **6b**−**e** can be synthesized best by the reaction of **5b** with an 1 molar equiv of LiR^3 (**9a**, R^3 = C≡C^{t}Bu, **9b**, R^3 = C≡CSiMe$_3$; **9c**, R^3 = C$_6$H$_2$(CF$_3$)$_3$-2,4,6; **9d**, R^3 = Me) in diethyl ether between −70 and 0 °C. While the reaction of **5b** with LiMe (**9d**) reacts spontaneously at low temperature, for all other reactions a longer reaction time is necessary (**9a**,**b** 1−2 h; **9c** 30 min), eq 4.

Thermolysis. When the gold−acetylide complexes **7** were heated in toluene to 80 °C, molecules **1** and **4a** are produced together with Au(0), eq 5. In this reaction the AuC≡CR^4 moieties undergo a reductive elimination

(11) Lang, H.; Frosch, W.; Wu, I. Y.; Blau, S.; Nuber, B. *Inorg. Chem.* **1996**, *35*, 6266.

(12) Köhler, K.; Pritzkow, H.; Lang, H. *J. Organomet. Chem.* **1997**, in press.

Table 1. Synthesis of Compounds 7a−e

compd	R^1	R^2	R^3	yield[a]
7a	$SiMe_3$	$SiMe_3$	$C{\equiv}CSiMe_3$	75%
7b	tBu	tBu	$C{\equiv}C^tBu$	76%
7c	$SiMe_3$	tBu	$C{\equiv}CSiMe_3$	60%
7d	$SiMe_3$	$SiMe_3$	$C_6H_2(CF_3)_3$-2,4,6	70%
7e	$SiMe_3$	$SiMe_3$	Me	60%

[a] On the basis of compounds **1a**−**c**.

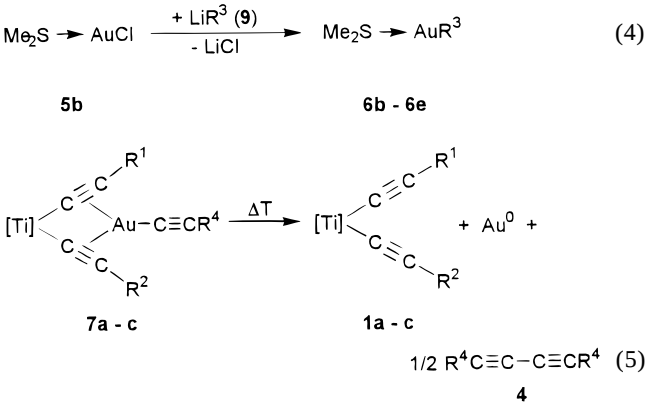

on formation of the appropriate 1,3-diynes $R^4C{\equiv}C-C{\equiv}CR^4$ (**4**), yielding Au(0). An analogous reaction behavior is found for heterobimetallic titanium−copper(I) acetylide complexes.[13]

The potential use of **7a**−**e** as precursors in the gold(I)−CVD process for the preparation of thin gold films is the subject of further research.

The bis(alkynyl) titanocenes $[Ti](C{\equiv}CR^1)(C{\equiv}CR^2)$ can be utilized for the stabilization of monomeric organogold(I) compounds, $\{[Ti](C{\equiv}CR^1)(C{\equiv}CR^2)\}AuR^3$, in which the gold atom possesses a trigonal-planar coordination sphere. The group 11 metal atom is σ-bonded by the organic ligand R^3, as well as complexed by the C≡C triple bond of the alkynyl ligands $C{\equiv}CR^1$ and $C{\equiv}CR^2$. These compounds allow one to study in detail monomeric organogold(I) compounds and provide information that is inaccessible from their polynuclear counterparts.

IR Studies. In agreement with the formulation of compounds **7** as heterobimetallic titanium−gold complexes in which both alkynyl ligands of the bis(alkynyl) titanocene fragment are η^2-coordinated to the appropriate organogold(I) moiety is the observation of a distinct C≡C stretching vibration in the IR spectra in the region of 1830−1896 cm^{-1}, indicating a weakening of the C≡C triple bonds on changing from the bis(alkynyl) titanocene parent compounds **1a**−**c** to the tweezer molecules **7a**−**e**. This shifting of the C≡C frequencies is similar to that observed for π-bonding of alkynes to group 11 metal moieties.[14] It is found that in the heterobimetallic complexes **7a**, **7d**, and **7e**, individual **7d** and **7e** show their ν(C≡C) vibration at lower wavenumbers (1830 cm^{-1}) than the gold−acetylide **7a** (1848 cm^{-1}). These data verify that a change of the η^1-bonded ligand R^3 in $\{[Ti](C{\equiv}C-SiMe_3)_2\}AuR^3$ from a weaker (**7a**) to a stronger (**7d**,**e**) σ-donor ligand leads to a weaker C≡C triple bond. As compared with isostructural organocopper(I) and -silver(I) compounds, $\{[Ti](C{\equiv}CSiMe_3)_2\}$-MR (M = Cu, Ag; R = singly-bonded organic ligand),[15] these data show that in the alkyne-to-metal interaction the C≡C triple bond is weakened more in the case of gold(I) than for copper(I) as well as silver(I) (*e.g.*, $\{[Ti](C{\equiv}CSiMe_3)_2\}MC_6H_2(CF_3)_3$-2,4,6; M = Au, 1830 cm^{-1}, M = Cu, 1877 cm^{-1}, M = Ag, 1930 cm^{-1}).[16] In this respect, the back-donation of filled metal orbitals into empty alkyne π^*-orbitals is stronger in the series gold > copper > silver.

Likewise, in the gold(I) acetylide complexes **7a**−**c**, a further ν(C≡C) vibration is found in the IR spectra at 2054 (**7a** and **7c**) or 2069 cm^{-1} (**7b**), in the region typical for η^1-bonded acetylide ligands.[14a,17]

^{1}H and ^{13}C{^{1}H} NMR Studies. The ^{1}H and ^{13}C NMR spectra of compounds **7a**−**e** consist of sharp and well-resolved resonance signals for each of the organic building blocks present. The most informative feature about the ^{1}H NMR spectra is the appearance of an AA′XX′ resonance pattern in the region of δ 4.9−5.8 with a coupling constant of J_{HH} = 2.3 Hz for compounds **7a**,**b**,**d**,**e**. In heterobimetallic **7c**, which contains two different alkynyl groupings, four pseudoquartets at δ 5.01, 5.10, 5.55, and 5.64 with J_{HH} = 2.5 Hz are observed, due to reduction of symmetry. Furthermore, it is found that compared with the bis(alkynyl) titanocene parent compounds **1a**−**c**, the resonance signals of the cyclopentadienyl entities in heterobimetallics **7a**−**e** are high-field-shifted. For isostructural $\{[Ti](C{\equiv}CSiMe_3)_2\}MC_6H_2(CF_3)_3$-2,4,6 (M = Cu, Ag, Au), a subsequent shift of the cyclopentadienyl proton resonance signals to higher field is noticed in the series of silver < copper < gold.[16]

In the ^{13}C{^{1}H} spectra it is found that upon the η^2-coordination of the C≡C triple bonds to the gold(I) center in complexes **7a**−**e**, the resonance signals of the C_α atoms in the $[Ti](C{\equiv}CR^1)(C{\equiv}CR^2)$ moieties are shifted downfield while the resonance signals of the C_β atoms are slightly shifted upfield. This finding is in agreement with an observation generally made by changing from noncoordinated to η^2-coordinated alkynyl substituted titanocenes.[13,14a,b,15,17b] The presence of two differently bonded alkynyl ligands (η^2-coordinated units in $[Ti](C{\equiv}CR^1)(C{\equiv}CR^2)$ and σ-bonded $C{\equiv}CR^4$ ligands in $AuC{\equiv}CR^4$) is evident by the observation of two further carbon resonance signals for the σ-bonded gold−alkynyl building block in the region of δ 91−130. In general, it is found that the carbon resonance signals of the noncoordinated $C{\equiv}CR^4$ groupings, as compared

(13) Lang, H.; Weinmann, M. *Synlett* **1996**, 1.
(14) (a) Lang, H.; Köhler, K.; Blau, S. *Coord. Chem. Rev.* **1995**, *143*, 113. (b) Lang, H.; Köhler, K.; Büchner, M. *Chem. Ber.* **1995**, *128*, 525. (c) Aalten, H. L.; van Koten, G.; Riethorst, E.; Stam, C. H. *Inorg. Chem.* **1989**, *28*, 4140. (d) Pasquali, M.; Leoni, P.; Floriani, C.; Gaetani-Manfredotti, A. *Inorg. Chem.* **1982**, *21*, 4324. (e) Olbrich, F.; Kopf, J.; Weiss, E.; Krebs, A.; Müller, S. *Acta Crystallogr.* **1990**, *C46*, 1650. (f) Maier, G.; Hoppe, H.; Reisenauer, H. P.; Krüger, K. *Angew. Chem.* **1982**, *94*, 445. (g) Schmidt, G.; Behrens, U. *J. Organomet. Chem.* **1996**, *509*, 49. (h) Chi, K. M.; Shin, H. K.; Hampden-Smith, M. J.; Kodas, T. T.; Duesler, E. N. *Inorg. Chem.* **1991**, *30*, 4293. (i) Chi, K. M.; Corbitt, T. S.; Hampden-Smith, M. J.; Kodas, T. T.; Duesler, E. N. *J. Organomet. Chem.* **1993**, *449*, 181.
(15) (a) Janssen, M. D.; Köhler, K.; Herres, M.; Dedieu, A.; Smeets, W. J. J.; Spek, A. L.; Grove, D. M.; Lang, H.; van Koten, G. *J. Am. Chem. Soc.* **1996**, *118*, 4817. (b) Janssen, M. D.; Herres, M.; Spek, A. L.; Grove, D. M.; Lang, H.; van Koten, G. *J. Chem. Soc., Chem. Commun.* **1995**, 925.
(16) Köhler, K.; Lang, H.; Zsolnai, L.; Büchner, M.; Driess, A.; Huttner, G. *Oganometallics*, submitted for publication.
(17) (a) Nakamoto, K. *Infrared and Raman-Spectra of Inorganic and Coordination Compounds*; Wiley Interscience: New York, 1977. (b) Janssen, M. D.; Herres, M.; Zsolnai, L.; Grove, D. M.; Spek, A. L.; Lang, H.; van Koten, G. *Organometallics* **1995**, *14*, 1098. (c) Vicente, J.; Chicote, M. T.; Abrisqueta, M. D. *J. Chem. Soc., Dalton Trans.* **1995**, 497.

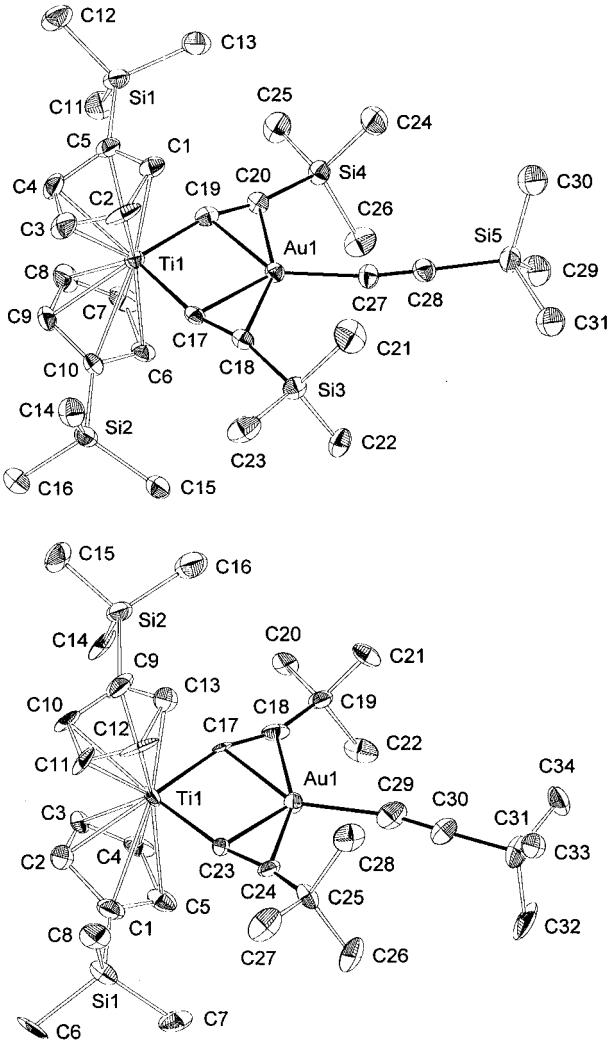

Figure 1. ORTEP drawings (drawn at 50% probability level) of **7a** (top) and **7b** (bottom) (with exclusion of the hydrogen atoms) with the atom-numbering schemes.

with the η^2-coordinated [Ti](C≡CR^1)(C≡CR^2) units, are shifted to higher field. In the monomeric gold(I) methyl compound **7e**, the carbon resonance signal of the methyl group could be detected at δ −10.3 and is, as compared with the appropriate resonance signals of the isostructural copper(I) and silver(I) methyl complexes, the most shifted to higher field.[15a,16]

X-ray Diffraction Studies. In order to establish the solid state structure of compounds **7a**−**e**, X-ray diffraction studies were carried out on single crystals of compounds **7a**,**b**,**d**. The structures of compounds **7a** and **7b** are shown in Figure 1, whereas the structure of heterobimetallic **7d** is depicted in Figure 2. Crystallographic parameters and selected geometrical details are listed in Tables 2−3.

In the unit cell of compound **7a** there is a molecule of toluene, and in the unit cell of **7b** a molecule of benzene is included. The structures of compounds **7a**,**b**,**d** are comprised of a trigonal-planar-coordinated gold atom η^2-coordinated by the alkynyl ligands of the bis(alkynyl) titanocene fragment and η^1-bonded by the appropriate singly-bonded organic ligands C≡CSiMe$_3$ (**7a**), C≡C-^{t}Bu (**7b**), or C$_6$H$_2$(CF$_3$)$_3$-2,4,6 (**7d**). The [Ti](C≡C)$_2$Au entity, as well as the gold-bonded carbon and/or silicon atoms of the η^1-bonded organic ligands (**7a**, C(27), C(28), Si(5); **7b**, C(29)−C(31); **7d**, C(25), C(28), C(32)) are in

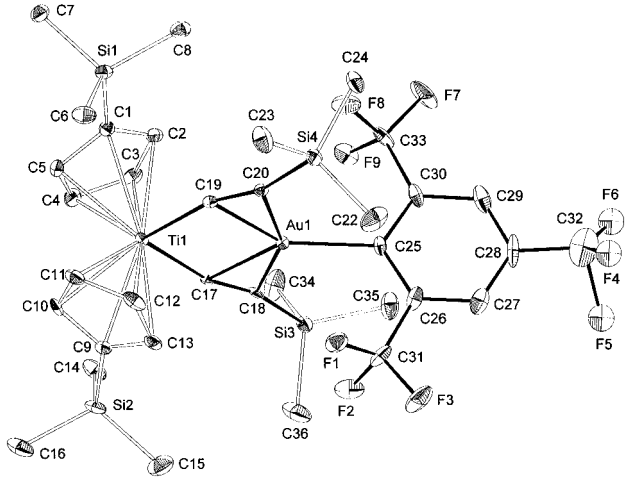

Figure 2. ORTEP drawing (drawn at 50% probability level) of **7d** (with exclusion of the hydrogen atoms) with the atom-numbering schemes.

the same plane (maximum atomic deviations are as follows: **7a**, 0.106 Å; **7b**, 0.104 Å; **7d**, 0.040 Å), which results in a trigonal-planar geometry of the group 11 metal atom. Consequently, the structure of the latter molecules contain a crystallographic 2-fold rotation axis that runs through Ti(1), Au(1), and the σ-bonded organic ligands (C(27), C(28), Si(5) for **7a**; C(29)−C(31) for **7b**; *ipso*-C(25), *para*-C(28), and *para*-CF$_3$, C(32), for **7d**). The plane of the η^1-bonded C$_6$H$_2$(CF$_3$)$_3$-2,4,6 ligand (C(25)−C(33)) in **7d** is almost perpendicular to the [Ti](C≡CSi)$_2$Au plane; the interplanar angle is 85.31°. As typical for tweezer molecules {[Ti](C≡CSiMe$_3$)$_2$}ML$_n$ (ML$_n$ = low-valent monomeric transition metal fragment), it is found that the monomeric AuR^3 entity in molecules **7a**−**e** is stabilized by the η^2-coordination of both alkynyl ligands of the seemingly bis(alkynyl) titanocene fragments **1a**−**c**. Likewise, the η^2-coordination results in a C≡C bond lengthening from 1.203(9)/1.214(6) Å in the starting compound **1a**[8a] to 1.26(1)/1.23(1) Å in **7a**, 1.236(7)/1.259(7) Å in **7b**, or 1.22(1)/1.25(1) Å in **7d**. In addition, a significant change of the initially linear arrangement of the Ti−C≡C−Si entities in compound **1a** is observed. The tweezer effect of the bis(alkynyl) titanocene induces a *trans*-deformation of the Ti−C≡C−Si moieties. While the Ti−C≡C and C≡C−Si angles are 175.8(4)/178.2(5)° and 174.6(4)/178.3(5)° in **1a**,[8a] these angles become much smaller in **7a** and **7d** (Ti(1)−C(17)−C(18), **7a** 162.4(8)°, **7d** 162.4(7)°; Ti(1)−C(19)−C(20), **7a** 163.6(9)°, **7d** 161.6(7)°; C(17)−C(18)−Si(3), **7a** 162.1(8)°, **7d** 155.3(7)°; C(19)−C(20)−Si(4), **7a** 162.1(9)°, **7d** 156.3(7)°), respectively. This *trans*-bending is typical for heterobimetallic compounds of the type {[Ti](C≡CSiMe$_3$)$_2$}ML$_n$.[13,14a] Through this deformation different gold-to-carbon bond lengths are observed (Table 3). The most striking feature about the η^2-coordination of the alkynyl ligands to the appropriate gold(I) entities is the decrease of the bite angle C−Ti−C′ from 102.8(2)° in the parent bis(alkynyl) titanocene compound **1a** to 95.5(4)° in **7a** and 95.4(3)° in **7d**, a phenomenon which is typical for tweezer like molecules.[13,14a] However, the angle D1−Ti−D2 (D1, D2 = centroids of the cyclopentadienyl ligands) in the bis(alkynyl) titanocene part is not influenced (Table 3).[13,14a] Similar observations were made for the ^{t}Bu-substituted heterobimetallic titanium−gold complex **7b** (Table 3). Moreover, the gold-titanium distances of 3.007(2) Å in

Table 2. Crystallographic Parameters for 7a, 7b, and 7d

	7a	7b	7d
formula	$C_{31}H_{53}AuSi_5Ti$	$C_{34}H_{53}AuSi_2Ti$	$C_{35}H_{46}AuF_9Si_4Ti$
fw	811.05	762.81	994.93
cryst syst	triclinic	triclinic	monoclinic
space group	$P\bar{1}$	$P\bar{1}$	$P2_1/c$
a, Å	10.946(4)	10.600(3)	15.730(4)
b, Å	11.195(4)	10.640(3)	12.959(2)
c, Å	19.59(1)	19.172(5)	20.334(3)
α, deg	105.62(3)	104.77(1)	
β, deg	100.12(2)	100.25(3)	88.35(1)
γ, deg	97.23(2)	95.61(3)	
V, Å^3	2237(2)	2034(1)	4143(1)
ρ_{calcd}, g cm^{-3}	1.272	1.319	1.595
Z	2	2	4
cryst size, mm^3	0.30 × 0.30 × 0.30	0.20 × 0.30 × 0.35	0.20 × 0.20 × 0.25
diff model	Siemens R3m/V	Siemens R3m/V	Siemens R3m/V
μ, mm^{-1}	3.61	3.88	3.91
radiation (λ, Å)	Mo Kα (0.710 73)	Mo Kα (0.710 73)	Mo Kα (0.710 73)
temp, K	200	200	200
scan mode	ω-scan	ω-scan	ω-scan
scan range $\Delta\omega$, deg	0.70	0.60	0.50
scan speed, deg min^{-1}	12.0−12.0	12.0−12.0	14.0−14.0
2θ range, deg	3.8−49.0	2.2−48.0	4.0−47.0
index range	$-1 \le h \le 12$	$0 \le h \le 12$	$-15 \le h \le 17$
	$-12 \le k \le 12$	$-11 \le k \le 11$	$-9 \le k \le 14$
	$-22 \le l \le 22$	$-21 \le l \le 21$	$-22 \le l \le 22$
no. of unique data	6577	6325	6119
no. of obsd data	5192 [$I \ge 2.0\sigma(I)$]	5707 [$I \ge 2.0\sigma(I)$]	4521 [$I \ge 2.0\sigma(I)$]
no. of refined params	411	383	460
R_1[a]	0.050	0.031	0.047
R_w[b]	0.135	0.084	0.106

[a] $R_1 = \sum||F_{obs}| - |F_{calc}||/\sum|F_{obs}|$. [b] $R_w = \{\sum[w(F_{obs}^2 - F_{calcd}^2)^2]/\sum[w(F_{obs}^2)^2]\}^{1/2}$.

Table 3. Selected Bond Lengths (Å) and Angles (deg) for Compounds 7a, 7b, and 7d

	7a	7b	7d
	Bond Lengths		
Ti−Au	3.007(2)	2.975(1)	2.995(1)
Au−C_{R3}	2.00(1)	2.018(6)	2.079(7)
Au−$C_{C\equiv C}$	2.228(9)	2.218(5)	2.217(7)
	2.23(1)	2.231(5)	2.245(7)
	2.255(9)	2.247(5)	2.217(8)
	2.27(1)	2.259(5)	2.245(8)
$C_\alpha \equiv C_\beta$	1.26(1)	1.236(7)	1.22(1)
	1.23(1)	1.259(7)	1.25(1)
	Angles		
Ti−$C_\alpha \equiv C_\beta$	163.6(9)	161.6(4)	162.1(6)
	162.4(8)	161.8(4)	162.4(7)
$C_\alpha \equiv C_\beta$−R	162.1(9)	159.1(5)	155.3(7)
	162.1(8)	159.4(5)	156.3(7)
Ti−Au−C_{R3}	176.8(3)	175.4(2)	179.4(2)
Au−C≡C	172(1)	172.5(5)	
C≡C−R^4	178(1)	177.5(6)	
C_α−Ti−$C_{\alpha'}$	95.5(4)	96.6(2)	95.4(3)
D1−Ti−D2[a]	134.4	133.8	134.6

[a] D1, D2 = centroids of the cyclopentadienyl ligands.

7a, 2.975(1) Å in **7b**, and 2.995(1) Å in **7d** are relatively short and suggest the possibility for a direct Ti−Au interaction.

Electronic Structure and Bonding. The electronic structure of {[Ti](C≡CSiMe$_3$)$_2$}MR complexes (M = group 11 metal atom, R = η^1-bonded organic ligand) has been recently discussed.[15a] On the basis of extended-Hückel analysis carried out for the molecular orbitals of the model compound [Cp$_2$Ti (C≡CH)$_2$]CuCH$_3$ (Cp = η^5-C$_5$H$_5$), it was pointed out that the stabilization of the MR monomers is dominated by the in-plane back-donation of electron density from the group 11 metal atom to the π^* orbital on the alkyne ligands. In spite of the relatively short Ti−M distances (M = Cu, Ag) observed experimentally, the Ti−M interactions have been considered to be nonbonding.[15a] Short Ti−Au contacts are also encountered in the case of compounds **7a**, **7b**, and **7d**. To find out whether or not Ti−Au interactions contribute to the stabilization of the Au−R^3 monomers, as well as to obtain insight into the nature of the Au−C bond, we have carried out extended-Hückel (EH) and density functional theory (DFT) calculations for the parent model compounds displayed in Scheme 3.

Scheme 3. Parent Model Compounds for Extended-Hückel (EH) and Density Functional Theory (DFT) Calculations

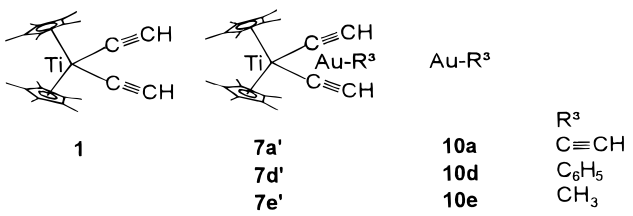

1 **7a'** **7d'** **7e'** **10a** **10d** **10e**

Bond distances and angles available from X-ray structure determinations were used for single-point DFT and EH calculations on **1**, **10a** and **7a′**.

Geometry optimizations of **10a**, **10d**, and **10e** as well as **7a′**, **7d′**, and **7e′** were carried out with the gradient technique at the DFT level. The computational details are described in the Experimental Section. First, we examine the electronic structure of **1**. We will focus on the shapes and energies of its frontier orbitals, since they will play a crucial role for the stabilization of organogold(I) monomers. We continue with an analysis of the bonding in **7e′** and finally we discuss the nature of the Au−C bond in the case of free and complexed Au−R^3 units.

Electronic Structure of Complex 1. To obtain an insight into the electronic structure of compound **1**, we adopted Hoffmann's fragment molecular orbital (MO)

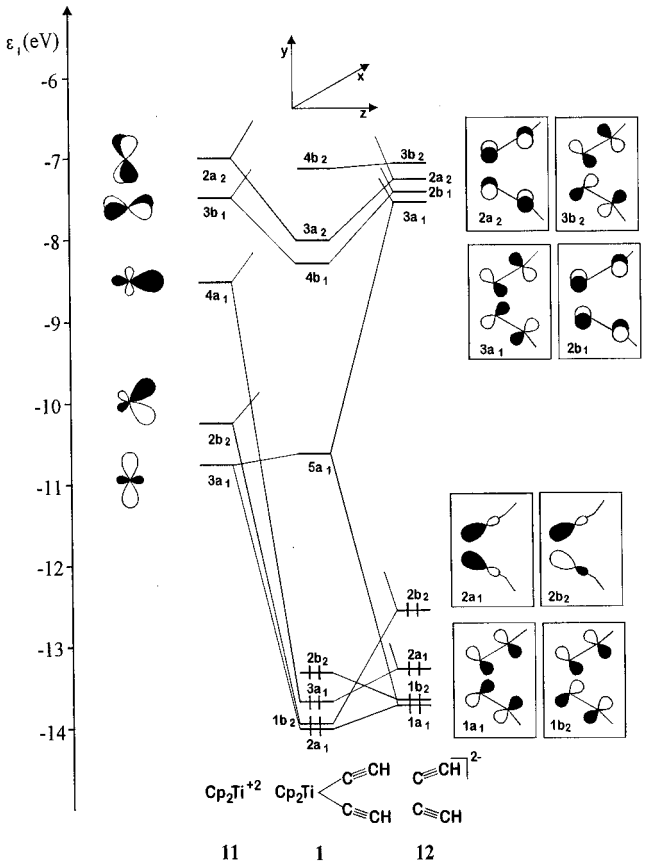

Figure 3. EH interaction diagram between the valence MOs of **11** and **12** to give **1**.

approach.[18] In Figure 3 we show the interaction diagram computed in C_{2v} symmetry with the EH method for the bonding between the metal fragment Cp_2Ti^{2+} (**11**) and the bis(acetylide) ligand $(C{\equiv}CH)_2^{2-}$ (**12**) to afford the titanocene **1**. The frontier orbitals of metallocene fragments are well-known; six occupied ligand-centered levels which are M−Cp bonding are followed by five MOs with predominant metal character.[18] Obviously, for the d^0 case of **11**, all metal levels are empty and can be involved in bonding interactions with occupied MOs of **12**. They are shown on the left side of Figure 3. The six ligand-centered levels do not contribute to the bonding with **12** and have been omitted. The valence MOs of **12**, shown on the right side of Figure 3, can be easily constructed as in-phase and out-of-phase combinations of the familiar valence MOs of two acetylide ligands. In our discussion, we use the labels $\pi_{||}$ and $\pi_{\perp}$, which refer to the in-plane and out-of-plane π MOs with respect to the $Ti(C{\equiv}CH)_2$ entity, *i.e.*, the *yz* plane of our coordinate system.

Among the frontier MOs of **12**, we have omitted the $1b_1$ and $1a_2$ combinations derived from occupied $\pi_{\perp}$ MOs. Due to the large energy gap and poor overlap with the $3b_1$ and $2a_2$ MOs of **11**, both combinations ($1b_1$, $1a_2$) are nonbonding and correlate with the $1a_2$ and $2b_1$ MOs of complex **1**. The shapes of these MOs are shown on the left side of Figure 4.

The in-plane interactions are only responsible for the bonding in **1**. Four donating MOs ($1a_1$, $2a_1$, $1b_2$, $2b_2$) of **12** interact with three low-lying accepting metal levels ($3a_1$, $2b_2$, $4a_1$) of **11** to produce the MOs of **1**. The

Scheme 4. LUMO ($5a_1$) (1) from [($3a_1$(11)-$1a_1$(12)]* and $3a_1$(12)

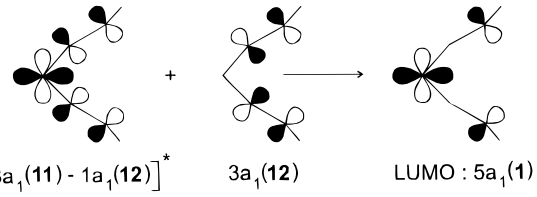

stabilization that results from these interactions can be inferred from the center of Figure 3. An examination of the MO shapes shows that LUMO + 2 ($4a_1$) and LUMO + 1 ($2b_2$) of **11** have good overlap with lone-pair MOs ($2a_1$, $2b_2$) of **12**. In the localized picture, the resulting $3a_1$ and $1b_2$ MOs of **1** describe the σ-bonds between the titanium atom and both alkyne ligands. The in-plane $1b_2$ ($\pi_{||}$) MO of **12** is also affected due to b_2 interactions and correlates with the $2b_2$ MO of complex **1**. From the interaction diagram it follows that the bonding of the acetylide ligands is supported by an additional interaction. The in-plane $1a_1$($\pi_{||}$) MO of **12** overlaps efficiently with the LUMO ($3a_1$) of **11** and produces the bonding $2a_1$ MO and the LUMO ($5a_1$) of **1**. As a consequence of this interaction, the Ti−C σ-bonds of **1** show some double-bond character. This statement is supported by the X-ray data from **1a** and $Cp_2Ti(CH_3)_2$. With respect to the bis(methyl) titanocene, the Ti−C_α bond distances of **1a** are shorter by 0.067/0.057 Å.[8,19]

The LUMO ($5a_1$) of **1** is low in energy, due to the bonding admixture of the empty $3a_1$ MO of **12** and $4a_1$ MO of **11**. Both admixtures are crucial because they rehybridize the metal contribution, change the shape of the LUMO, and lead to a partial relief of antibonding interactions, as shown in Scheme 4. The shape of the low-lying, electrophilic LUMO ($5a_1$) suggests that the C_α atoms of the acetylide ligands should be unaffected by back-bonding interactions from nucleophilic fragments. An electron density transfer can be expected for the in-plane orbitals of the Ti and C_β atoms of the acetylide ligands (Scheme 4).

Bonding in Complex 7a′. The bonding in the dinuclear complex **7a′** can be analyzed in a similar manner. The interaction diagram computed in C_{2v} symmetry is shown in Figure 4. For the bonding with the bis(alkynyl) titanocene building block **1**, fragment **10a** provides six occupied levels. The shapes of these MOs together with the LUMO of σ^*(Au−C) character are depicted on the right side of Figure 4. For the sake of clarity, in Figure 4 we have omitted the π MOs of the acetylide ligand from **10a** as well as the $1b_2$ and $3a_1$ MOs of **1**, which describe the Ti−C_α σ-bonds (cf. Figure 3). These MOs do not contribute to the bonding interactions.

The Au $d_\pi(xz,yz)$ and $d_\delta(xy)$ levels are close in energy to the occupied $1a_2$, $2b_1$, and $2b_2$ MOs of **1** and give rise to repulsive two-orbital four-electron interactions. A reduction of these destabilizing effects is possible by an admixture of the empty MOs ($3a_2$, $4b_1$, $4b_2$) of **1** to form three-orbital four-electron interactions of generally bonding character. An electron density shift is possible from the Au d_{xz}, d_{yz}, and d_{xy} orbitals to the acetylide out-of-plane ($4b_1$, $3a_2$) and in-plane ($4b_2$) π^* MOs of **1**. The

(18) Albright, T. A.; Burdett, J. K.; Whangbo, M.-H. *Orbital Interactions in Chemistry*; Wiley: New York, 1985.

(19) Thewalt, U.; Wöhrle, T. *J. Organomet. Chem.* **1994**, *464*, C17.

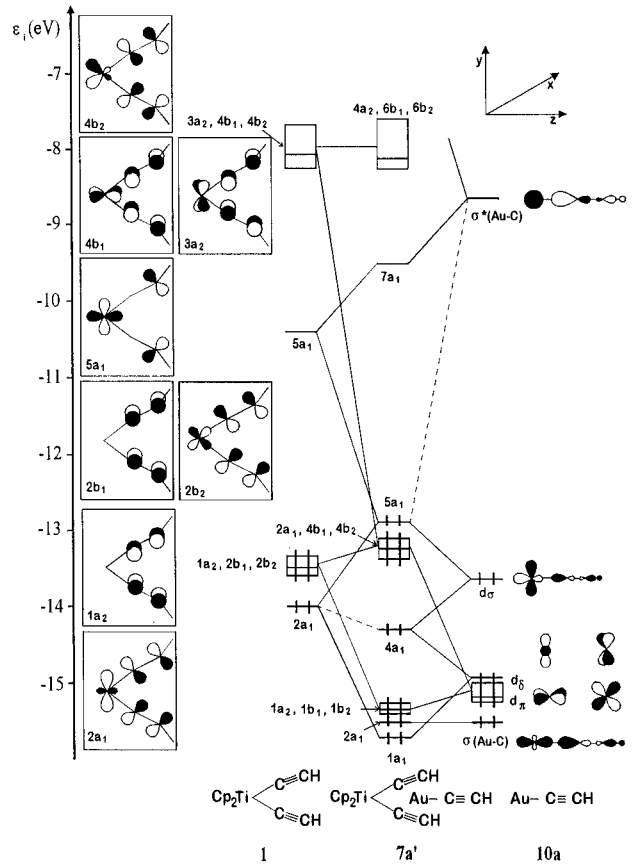

Figure 4. EH interaction diagram between the valence MOs of **1** and **10a** to give **7a′**.

Scheme 5. Mixing Pattern of [(2a$_1$(1)-Au: d$_\sigma$ (10a)]* and LUMO (5a$_1$) (1) To Give 5a$_1$(7a′)

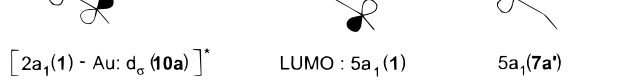

bonding between a_1 MOs is slightly more complex, since both fragments provide occupied and empty levels for a_1 interactions. The strongest repulsive interaction takes place between 2a$_1$($\pi_{||}$) MO of **1** and Au d$_\sigma$ of **10a**. The resulting 5a$_1$ MO of **7a′** corresponds to the antibonding component of this interaction. However, the bonding admixture of the LUMO (5a$_1$) of **1** compensates for the repulsive interactions and transforms the 5a$_1$ MO of **7a′** to a four-center bonding level. The corresponding mixing pattern is displayed in Scheme 5.

The shape of the 5a$_1$ MO of **7a′** clearly demonstrates that the Ti−Au overlap contributes to the stabilization of this four-center two-electron bond. Furthermore, from the interaction diagram it follows that the 5a$_1$ MO of **7a′** receives some stabilization from the LUMO of **10a** (Figure 4).

Thus, for a_1 interactions a synergetic donation and back-donation of electron density is possible, *i.e.*, from the 2a$_1$ ($\pi_{||}$) MO of **1** to the LUMO of **10a** and from Au d$_\sigma$ to the LUMO of **1**. The ratio of the density shift in this donation and back-donation interactions cannot be inferred from the interaction diagram. In order to quantify these donor−acceptor interactions, the DFT wave functions of **1**, **10a**, and **7a′** were localized to give natural atomic orbitals (NAOs) and natural bond orbitals (NBOs). The results of the population analysis carried out for the localized wave functions are summarized in Tables 4 and 5.

Table 4. Occupation Numbers of the Particular NBOs of 1, 10a, and 7a′

	occupancy				
NBO	**10a**	**7a′**	NBO:C≡C	**1**	**7a′**
$d_\delta(x^2-y^2)$	2.000	1.993[a]			
$d_\delta(xy)$	2.000	1.997			
$d_\pi(xz)$	1.977	1.967	$\pi_\perp$*	0.022	0.031
$d_\pi(yz)$	1.977	1.902			
$d_\sigma(z^2-y^2)$	1.997	1.658	$\pi_{||}$*	0.015	0.187
σ(Au−C)	1.993	1.855			
σ*(Au−C)	0.014	0.194	$\pi_{||}$	1.889	1.750
			$\pi_\perp$	1.967	1.969

[a] In **7a′**, the character of this NBO changes to d($z^2 - x^2$).

Table 5. Intergrated Natural Atomic Charge of Molecular Fragments in 1, 10a, and 7a′

fragment	**1**	**7a′**	fragment	**10a**	**7a′**
Ti	+0.394	+0.134	Au	+0.423	+0.956
C_5H_5	+0.103	+0.129	$C_{\alpha'} \equiv C_{\beta'}H$	−0.423	−0.598
$C_\alpha \equiv C_\beta H$	−0.300	−0.375	$C_{\alpha'}$	−0.377	−0.479
C_α	−0.271	−0.283	$C_{\beta'}$	−0.285	−0.342
C_β	−0.256	−0.359	**10a**	0.000	+0.358
1	0.000	−0.358			

An out-of-plane back-donation of electron density from Au d$_\delta$(xy) and d$_\pi$(xz) orbitals to the $\pi_\perp$* NBOs of **1** is not important for the stabilization of **10a**. With respect to the molecular fragments **1** and 1**0a**, the occupancy of these out-of-plane NBOs does not change significantly in **7a′** (Table 4).

Strong density shifts are calculated for in-plane interactions. The occupancy of $\pi_{||}$ NBOs of **1** diminishes from 1.889 (**1**) to 1.750 Å (**7a′**) and those of σ*(Au−C) NBO increases from 0.014 (**10a**) to 0.194 Å (**7a′**). Due to back-bonding from Au d$_\sigma$($z^2 - y^2$), σ(Au−C), and d$_\pi$(yz) NBOs, the occupancy of $\pi_{||}$* NBOs of **1** increases from 0.015 (**1**) to 0.187 Å (**7a′**). It is clear that on changing from **1** to **7a′**, a population of $\pi_{||}$* NBOs, as well as depopulation of $\pi_{||}$ NBOs, will weaken the C≡C (Ti−C≡C) triple bonds. This finding is in accord with the IR data known for this class of compounds and explains the observed shifting of the C≡C frequencies to lower wavenumbers in the heterobimetallic compounds. The strongest back-bonding is calculated for the Au d$_\sigma$($z^2 - y^2$) NBO, but the σ(Au−C) NBO is also involved in these interactions. Again, the calculated depopulation for **7a′** of the σ(Au−C) NBO as well as the population of its antibonding counterpart weakens the Au−C bond. Note, that thermolysis reactions discussed in this paper produce Au(0) together with bis(alkynyl) titanocene and the corresponding RC≡C−C≡CR compounds. Additional information concerning the bonding in **7a′** can be obtained by a comparison of the integrated natural atomic charges for molecular fragments of **1** and **10a** with those of **7a′**. These results have been summarized in Table 5. The reorganization of the electron density in **7a′** is dominated by back-bonding. In **7a′**, 0.358 e are transferred from **10a** to **1.** With respect to **1**, the electron density accompanying the titanium atom in **7a′** increases by 0.26 e and that of one acetylide ligand by 0.075 e (Table 5).

The increase of electron density on the C_α atoms is insignificant (−0.271 e in **1** and −0.283 e in **7a′**), but

Table 6. Calculated Au−C Bond Lengths (Å) and Results of the NBO Population Analysis[a]

	d_{Au-C} (X)				OCC		% Au				
compd	calcd	exp[b]	q Au	q C	σ_{Au-C}	σ^*_{Au-C}	σ_{Au-C}	σ^*_{Au-C}	%s Au	%p Au	%d Au
10a	1.931		+0.42	−0.39	1.993	0.015	31.8	68.2	84.4	0.2	15.4
10d	2.014		+0.22	−0.21	1.964	0.050	40.7	59.3	80.2	0.1	19.7
10e	2.049		+0.18	−0.87	1.999	0.008	42.3	57.7	80.9	0.0	19.1
7a′	2.004	2.001/2.018	+0.82	−0.48	1.904	0.153	21.5	78.5	92.1	0.0	7.9
7d′	2.071	2.079	+0.81	−0.36	1.807	0.158	24.4	75.6	91.4	0.1	8.5
7e′	2.110		+0.77	−1.03	1.829	0.139	26.7	73.3	91.4	0.3	8.3

[a] q Au and q C give the natural atomic charge for the atoms of the Au−C bonds; OCC gives the occupancy for the Au−C σ and σ^* NBOs; % Au gives overall Au contribution for the Au−C σ and σ^* NBOs; %s Au, %p Au, and %d Au give the hybridization of Au in Au−C σ and σ^* NBOs. [b] X-ray crystal data, this work.

that for C_β atoms amounts to 0.103 e. This finding is in agreement with the upfield shift of the resonance signal of the C_β atoms observed in the $^{13}C\{^1H\}$ NMR spectra of heterobimetallic compounds. The downfield shift of the ^{13}C NMR signal of the C_α atoms still remains unclear, according to our population analysis. We suppose that calculations with more flexible basis sets and a direct theoretical estimation of the NMR spectra of the molecules investigated may clarify this discrepancy. Due to the size of the complexes, such investigations are rather time consuming and were not undertaken for the present studies. Nevertheless, the results of the population analysis clearly show that the stabilization of **10a** is dominated by an in-plane back-donation of electron density from Au to the Ti and C_β atoms of complex **1**. A direct donor−acceptor Au−Ti interaction contributes to this stabilization.

Nature of the Au−C Bond. The optimized Au−C bond lengths together with results of the NBO population analysis are collected in Table 6. The optimized Au−C bond distances of **7a′** and **7d′** agree very well with the X-ray values of **7a** and **7d.** To our knowledge, the X-ray data for **10a**, **10d**, and **10e** are not known. However, we notice that the optimized Au−C bond length of **10d** and **10e** agrees within 0.03 Å with the MP2 (Møller−Plesset perturbation theory terminated at second order) values calculated by Antes and Frenking with a Stoll and Preuss pseudopotential for the Au atom.[20] For the Au−R^3 monomers, our results predict an elongation of the Au−C bond in the order Au−C(sp) < Au−C(sp^2) < Au−C(sp^3). This is reasonable considering not only the hybridization of the carbon atom, but also the fact that back-bonding interactions from Au to R^3 are not possible for **10e**. The complexation of Au−R^3 monomers leads to an elongation of the Au−C bond by 0.073 (**7a′**), 0.057 (**7d′**), and 0.061 Å (**7e′**) (Table 6). As discussed in the previous section, this elongation has its origin in the donation of electron density from the acetylide ligands of **1** to the σ^*(Au−C) bond and in the back-bonding component from the σ(Au−C) bond to the LUMO of **1**. The Au−C bonds are polarized toward the carbon end, and consequently, the corresponding σ^* bonds are polarized toward the metal. This becomes evident by the calculated charge at the gold atom (q Au) and the overall Au contribution to the Au−C σ and σ^* bonds. The polarization of the Au−C bond of **10a** is higher than that of **10d** and **10e**. The Au−C(sp^3) and Au−C(sp^2) bonds of **10e** and **10d** are clearly more covalent than the Au−C(sp) bond of **10a**. The total Au contribution to the Au−C bonds in Au−R^3 monomers (31.8%, **10a**; 40.7%, **10d**; 42.3%, **10e**) has a large s(Au) character, but the d(Au) character is not negligible for these bonds (15.4%, **10a**; 19.7%, **10d**; 19.1%, **10e**). Due to complexation with **1**, the polarization of the Au−C bonds increases and at the metal end these bonds have nearly pure s(Au) character with very little d(Au) contribution (7.9%, **7a′**; 8.5%, **7d′**; 8.3%, **7e′**).

For complexed Au−R^3 molecules, the increase in the polarity of the Au−C(sp^3) and Au−C(sp^2) bonds is greater than that of the Au−C(sp) bond. Thus, in **7a′**, **7d′**, and **7e′** independent of the hybridization of the carbon atom, either of the Au−C bonds has a large polar character.

(20) Antes, I.; Frenking, G. *Organometallics* **1995**, *14*, 4263.

Experimental Section

General Comments. All reactions were carried out under an atmosphere of nitrogen using standard Schlenk techniques. Diethyl ether and *n*-pentane were purified by distillation from calcium hydride. Infrared spectra were obtained with a Perkin-Elmer 983G spectrometer. ^1H NMR spectra were recorded on a Bruker AC 200 spectrometer operating at 200.132 MHz in the Fourier transform mode, and the $^{13}C\{^1H\}$ NMR spectra were recorded at 50.323 MHz. Chemical shifts are reported in δ units (parts per million) downfield from tetramethylsilane with the solvent as the reference signal. EI mass spectra were recorded on a Finnigan 8400 mass spectrometer operating in the positive-ion mode. Melting points were determined with the use of analytically pure samples, which were sealed in nitrogen-purged capillaries on a Gallenkamp MFB 595 010 M melting point apparatus. Microanalyses were performed by the Organisch-Chemisches Institut der Universität Heidelberg.

Synthesis of Compounds 7a−d. A 0.39 mmol sample of HR^3 (R^3 = C≡CSiMe$_3$, 40 mg; R^3 = C≡C^{t}Bu, 32 mg; R^3 = $C_6H_2(CF_3)_3$-2,4,6, 110 mg) was metalated at 0 °C in diethyl ether (50 mL) with ^{n}BuLi (0.17 mL, 0.39 mmol, 2.3 M ^{n}BuLi/hexane). After the mixture was stirred for 1 h, (Me_2S)AuCl (**5b**)[5g] (115 mg, 0.39 mmol) was added. After precipitation of LiCl, the compounds (Me_2S)AuR^3 (**6b**, R^3 = C≡CSiMe$_3$; **6c**, R^3 = C≡C^{t}Bu; **6d**, R^3 = $C_6H_3(CF_3)_3$-2,4,6) was formed. After 30 min, the reaction mixture obtained was treated with 0.39 mmol of [Ti](C≡CR^1)(C≡CR^2) (**1a**, R^1 = R^2 = SiMe$_3$,[8] 200 mg; **1b**, R^1 = R^2 = ^{t}Bu,[8] 190 mg; **1c**, R^1 = SiMe$_3$, R^2 = ^{t}Bu,[10a] 195 mg). After the mixture was stirred for 2 h at 25 °C, all volatile materials were removed in vacuo and the residue was extracted with 50 mL of *n*-pentane and filtered through a pad of Celite. The solution was concentrated to yield pale orange crystals of **7a−d** upon cooling to 0 °C in 60−80% yield (Table 1).

Data for **7a**: mp 105 °C (dec); IR (KBr, ν(C≡C), cm^{-1}) 2054 (s, AuC≡CSiMe$_3$), 1848 (m, η^2-TiC≡CSiMe$_3$); ^1H NMR (C_6D_6) δ 0.20 (s, 18 H, SiMe$_3$), 0.39 (s, 9 H, SiMe$_3$), 0.63 (s, 18 H, SiMe$_3$), 4.94 (pt, 4 H, C_5H_4, J_{HH} = 2.3 Hz), 5.58 (pt, 4 H, C_5H_4, J_{HH} = 2.3 Hz); ^{13}C NMR (C_6D_6) δ 0.6 (SiMe$_3$), 1.0 (SiMe$_3$), 1.5 (SiMe$_3$), 110.4 (C_5H_4), 113.2 (C_5H_4), 116.9 ($^iC-C_5H_4$), 122.0 (C≡*C*Si), 123.4/129.6 (Au*C*≡*C*SiMe$_3$), 181.1 (Ti*C*≡C); EI MS, *m*/*e* (relative intensity) 810 (M^+, 20), 613 ($M^+ - 2C_2SiMe_3$, 40), 418 ($M^+ - AuC_2SiMe_3 - C_2SiMe_3$, 5), 322 ((($C_5H_4SiMe_3$)$_2$-

Ti^+, 322 100), 73 ($SiMe_3^+$, 25). Anal. Calcd for $C_{31}H_{53}AuSi_5Ti$ (811.05): C, 45.90; H, 6.59. Found: C, 45.79; H, 6.83.

Data for **7b**: mp 81 °C (dec); IR (KBr, ν(C≡C), cm^{-1}) 2069 (w, AuC≡C^{t}Bu), 1896 (w, η^2-TiC≡C^{t}Bu); ^{1}H NMR (C_6D_6) δ 0.23 (s, 18 H, $SiMe_3$), 1.53 (s, 9 H, ^{t}Bu), 1.73 (s, 18 H, ^{t}Bu), 5.13 (pt, 4 H, C_5H_4, J_{HH} = 2.3 Hz), 5.58 (pt, 4 H, C_5H_4, J_{HH} = 2.3 Hz); ^{13}C NMR (C_6D_6) δ 0.6 ($SiMe_3$), 31.5 (*C*Me_3), 32.0 (C*Me*$_3$), 91.7/118.3 (Au*C*≡*C*^{t}Bu), 110.5 (C_5H_4), 113.5 (C_5H_4), 114.6 (^{i}C−C_5H_4), 138.5 (C≡*C*CMe_3), 152.1 (Ti*C*≡C); EI MS *m*/*e* (relative intensity) 762 (M^+, 30), 680 ($M^+ - C_2{}^t$Bu, 100), 600 ($M^+ - 2C_2{}^t$Bu, 50), 402 ($M^+ - AuC_2{}^t$Bu − $C_2{}^t$Bu, 50). Anal. Calcd for $C_{34}H_{53}AuSi_2Ti$ (762.81): C, 53.53; H, 7.00. Found: C, 53.70; H, 7.37.

Data for **7c**: mp 98 °C (dec); IR (KBr, ν(C≡C), cm^{-1}) 2054 (s, AuC≡C$SiMe_3$), 1881 (w, η^2-TiC≡C^{t}Bu), 1848 (w, η^2-TiC≡C$SiMe_3$); ^{1}H NMR (C_6D_6) δ 0.22 (s, 18 H, $SiMe_3$), 0.44 (s, 9 H, $SiMe_3$), 0.69 (s, 9 H, $SiMe_3$), 1.70 (s, 9 H, ^{t}Bu), 5.01 (pq, 2 H, C_5H_4, J_{HH} = 2.5 Hz), 5.10 (pq, 2 H, C_5H_4, J_{HH} = 2.5 Hz), 5.55 (pq, 2 H, C_5H_4, J_{HH} = 2.5 Hz), 5.64 (pq, 2 H, C_5H_4, J_{HH} = 2.5 Hz); ^{13}C NMR (C_6D_6) δ 0.6 ($SiMe_3$), 1.0 ($SiMe_3$), 1.5 ($SiMe_3$), 31.4 (*C*Me_3), 32.0 (C*Me*$_3$), 110.3 (C_5H_4), 110.7 (C_5H_4), 113.0 (C_5H_4), 113.4 (C_5H_4), 116.1 (^{i}C−C_5H_4), 123.0 (TiC≡*C*Si), 123.4/129.7 (Au*C*≡*C*$SiMe_3$), 139.1 (TiC≡*C*^{t}Bu), 152.4 (Ti*C*≡C^{t}Bu), 180.2 (Ti*C*≡C); FAB MS *m*/*e* (relative intensity) 795 (M^+, 40), 713 ($M^+ - C_2{}^t$Bu, 20), 418 ($M^+ - AuC_2{}^t$Bu − $C_2{}^t$Bu, 100). Anal. Calcd for $C_{32}H_{53}AuSi_4Ti$ (794.97): C, 48.34; H, 6.72. Found: C, 48.21; H, 6.83.

Data for **7d**: mp 118 °C (dec); IR (KBr, ν, cm^{-1}) 1830 (C≡C); ^{1}H NMR (C_6D_6) δ 0.04 (s, 18 H, $SiMe_3$), 0.27 (s, 18 H, $SiMe_3$), 5.22 (pt, 4 H, C_5H_4, J_{HH} = 2.3 Hz), 5.75 (pt, 4 H, C_5H_4, J_{HH} = 2.3 Hz), 8.17 (s, 2 H, C_6H_2); ^{13}C NMR (C_6D_6) δ 0.5 ($SiMe_3$), 0.7 ($SiMe_3$), 111.1 (C_5H_4), 113.0 (C_5H_4), 116.5 (^{i}C−C_5H_4), 123.5 (C≡*C*Si), 123.8 (*m*-C_6H_2), 124.4 (AuC), 139.9 (q, ^{i}C−C_6H_2, $^2J_{CF}$ = 28.4 Hz), 183.5 (Ti*C*≡C), CF_3 could not unambiguously be assigned; EI MS *m*/*e* (relative intensity) 994 (M^+, 40), 616 ($M^+ - C_6H_2(CF_3)_3 - C_2SiMe_3$, 55), 516 ($M^+ - AuC_6H_2(CF_3)_3$, 45), 322 (($C_5H_4SiMe_3)_2Ti^+$, 100). Anal. Calcd for $C_{35}H_{46}AuF_9Si_4Ti$ (994.93): C, 42.25; H, 5.66. Found: C, 43.05; H, 4.95.

Synthesis of Compound 7e. To (Me_2S)AuCl (**5b**)[5g] (115 mg, 0.39 mmol) in 50 mL of diethyl ether was added at −60 °C LiMe (0.24 mL, 0.39 mmol, 1.6 M LiMe/diethyl ether) in one portion. After 1 min, the reaction mixture obtained was treated with [Ti](C≡C$SiMe_3)_2$ (**1a**)[8] (200 mg, 0.39 mmol). After the mixture was stirred for 2 h at 0 °C, all volatile materials were removed in vacuo and the residue was extracted with 50 mL of *n*-pentane and filtered through a pad of Celite. The solution was concentrated to a yield pale orange solid of **7e** upon cooling to −30 °C in 60% yield: mp 55 °C (dec); IR (KBr, ν, cm^{-1}) 1831 (C≡C); ^{1}H NMR (C_6D_6) δ 0.27 (s, 18 H, $SiMe_3$), 0.46 (s, 18 H, $SiMe_3$), 1.70 (s, 3 H, Me), 4.97 (pt, 4 H, C_5H_4, J_{HH} = 2.3 Hz), 5.61 (pt, 4 H, C_5H_4, J_{HH} = 2.3 Hz); ^{13}C NMR (C_6D_6) δ −10.3 (AuMe), 0.6 ($SiMe_3$), 1.1 ($SiMe_3$), 109.0 (C_5H_4), 112.3 (C_5H_4), 115.9 (^{i}C−C_5H_4), 122.6 (C≡*C*Si), 199.1 (Ti*C*≡C). Anal. Calcd for $C_{27}H_{47}AuSi_4Ti$ (728.88): C, 44.49; H, 6.50. Found: C, 44.01; H, 6.38.

X-ray Structure Determination of 7a, 7b, and 7d. The structures of compounds **7a, 7b**, and **7d** were determined from single-crystal X-ray diffraction data, which were collected using a Siemens R3m/V (Nicolet Syntex) diffractometer. Crystallographic data for **7a, 7b**, and **7d** are given in Table 2. All structures were solved by direct methods (Sheldrick, G. M. *SHELXTL PLUS*; University of Göttingen: Göttingen, Germany, 1988). An empirical absorption correction was applied. The structures were refined by the least-squares method based on F^2 with all reflections (Sheldrick, G. M. *SHELXL 93*; University of Göttingen: Göttingen, Germany, 1993). All non-hydrogen atoms were refined anisotropically; the hydrogens were placed in calculated positions.

Theoretical Studies. For DFT[21] calculations, we used the hybrid method with Becke's three-parameter functional approach[22] and the correlation potentials of Lee, Yang, and Parr.[23] A single basis set was applied in our studies. The all-electron basis sets of respective sizes (10s, 5p) and (4s) were used for carbon and hydrogen and contracted to split valence.[24] The core electrons of the metals were replaced by nonrelativistic (Ti) and relativistic (Au) pseudopotentials.[25] For both metals, we utilized the small-core approximation, *i.e.*, the valence space of the metals is augmented by the outermost (n − 1)s^2(n − 1)p^6 core electrons. This means that the 12 valence electrons of Ti and 19 valence electrons of Au are calculated explicitly. For these electrons we applied the [341/311/41] and [341/321/21] basis sets of Hay and Wadt, respectively.[25] The contraction schemes correspond to a single-ξ description for the outermost core electrons and to a double-ξ description for the valence electrons. The description of the bonding situation in the investigated molecules has been carried out by means of the natural bond orbital (NBO) and natural atomic orbital (NAO) population analysis[26] applied to the DFT wave functions, as well as by means of the extended-Hückel (EH) method.[27] The EH calculations were carried out with standard parameters for all atoms.[27d,28] The calculations have been carried out using the program packages Gaussian 94[29] and Molek-9000.[30]

Acknowledgment. We are grateful to the Deutsche Forschungsgemeinschaft (Grant No. SFB 247), the Fonds der Chemischen Industrie, and the Hermann-Schlosser Stiftung Degussa AG Frankfurt (K.K.) for financial support. We are grateful to Prof. Dr. Dr. h.c. H. W. Roesky for a generous gift of $C_6H_3(CF_3)_3$-1,3,5. We thank Th. Jannack for carrying out the MS measurements and Dr. Dr. Ch. Limberg as well as S. Ahrens for fruitful discussions.

Supporting Information Available: Tables of crystal data and structure refinement, bond lengths and bond angles, and anisotropic displacement factors for **7a**, **7b**, and **7d** (12 pages). Ordering information is given on any current masthead page.

OM970302I

(21) Parr, R. G.; Yang, W. *Density Functional Theory of Atoms and Molecules*; Oxford University Press: Oxford, 1989.
(22) Becke, A. D. *J. Chem. Phys.* **1993**, *98*, 5648.
(23) Lee, C.; Yang, W.; Parr, R. G. *Phys. Rev. B* **1988**, *37*, 785.
(24) Dunning, T. H.; Hay, J. P. *Modern Theoretical Chemistry*; Plenum: New York, 1976; Chapter 1.
(25) Hay, J. P.; Wadt, W. R. *J. Chem. Phys.* **1985**, *82*, 299.
(26) (a) Foster, J. P.; Weinhold, F. *J. Am. Chem. Soc.* **1980**, *102*, 7211. (b) Reed, A. E.; Weinhold, F. *J. Chem. Phys.* **1983**, *78*, 4066. (c) Reed, A. E.; Curtiss, L. A.; Weinhold, F. *Chem. Rev.* **1988**, *88*, 899.
(27) (a) Hoffmann, R.; Lipscomb, W. N. *J. Chem. Phys.* **1962**, *36*, 2179. (b) Ibid. **1962**, *36*, 3488. (c) Ibid. **1962**, *37*, 2872. (d) Hoffmann, R. Ibid. **1963**, *39*, 1397.
(28) (a) Komiya, S.; Albright, T. A.; Hoffmann, R.; Kochi, J. K. *J. Am. Chem. Soc.* **1977**, *99*, 8440. (b) Lauher, J. W.; Hoffmann, R. *J. Am. Chem. Soc.* **1976**, *98*,1729.
(29) Frisch, M. J.; Trucks, G. W.; Schlegel, H. B.; Gill, P. M. W.; Johnson, B. G.; Robb, M. A.; Cheeseman, J. R.; Keith, T.; Petersson, G. A.; Montgomery, J. A.; Raghavachari, K.; Al-Laham, M. A.; Zakrzewski, V. G.; Oritz, J. V.; Foresman, J. B.; Cioslowski, J.; Stefanov, B. B.; Nanayakkara, A.; Challacombe, M.; Peng, C.Y.; Ayala, P. Y.; Chen, W.; Wong, M. W.; Andres, J. L; Replogle, E. S.; Gomperts, R.; Martin, R. L.; Fox, D. J.; Binkley, J. S.; Defrees, D. J.; Baker, J.; Stewart, J. P.; Head-Gordon, M.; Gonzales, C.; Pople, J. A. *Gaussian 94, revision D.2*; Gaussian, Inc.: Pittsburgh, PA, 1995.
(30) Bischof, P. *Molek-9000*; Organisch-Chemisches Institut, Universität Heidelberg, Heidelberg, Germany.